Mineralogical Magazine, February 2001, Vol. 65(1), pp. 41–58

A high-pressure structural study of lawsonite using angle-dispersive powder-diffraction methods with synchrotron radiation

A. R. PAWLEY[1] AND D. R. ALLAN[2]

[1] Department of Earth Sciences, University of Manchester, Oxford Road, Manchester M13 9PL, UK
[2] Department of Physics and Astronomy, University of Edinburgh, Mayfield Road, Edinburgh EH9 3JZ, UK

ABSTRACT

Structural refinements of lawsonite have been obtained at pressures up to 16.5 GPa using angle-dispersive powder diffraction with synchrotron radiation on a natural sample contained in a diamond anvil cell. Lawsonite compresses smoothly and relatively isotropically up to 10 GPa. Its bulk modulus is 126.1(6) GPa (for $K' = 4$), consistent with previous results. A trend of decreasing Si–O–Si angle indicates that compression is accommodated partly through the narrowing of the cavities containing Ca and H_2O in the $[001]_{ortho}$ direction. At 10–11 GPa there is a phase transition from *Cmcm* to $P2_1/m$ symmetry. The occurrence of a mixed-phase region, spanning >1 GPa, indicates that the transition is first order in character. The phase transition occurs through a shearing of $(010)_{ortho}$ sheets containing AlO_6 octahedral chains in the $[100]_{ortho}$ direction, which causes an increase in β_{mono}. Across the transition, the number of oxygens coordinated to Ca increases from 8 to 9, causing an increase in the average Ca–O bond length. The compressibility of $P2_1/m$ lawsonite could not be determined due to solidification of the methanol/ethanol pressure-transmitting medium. On the basis of an experiment in which the $P2_1/m$ lawsonite structure was heated to 200°C at 12.0 GPa, we predict a shallow positive *P-T* slope for the phase transition, and therefore no stability field for $P2_1/m$ lawsonite in the Earth.

KEYWORDS: lawsonite, high-pressure, phase transition, synchrotron radiation, powder diffraction.

Introduction

LAWSONITE, $CaAl_2Si_2O_7(OH)_2{\cdot}H_2O$, is an important water-rich mineral that crystallizes in high-pressure metamorphic rocks. It is most common in blueschist-facies metabasalts and metagreywackes, and has also been found in metapelites and in eclogite-facies metabasalts. Blueschist- and eclogite-facies metamorphism occurs when oceanic lithosphere, variably capped by sediment, descends into the Earth's mantle at subduction zones. The oceanic crust is partially hydrated by hydrothermal alteration close to oceanic spreading centres, and the sediments are water-rich. Thus, new hydrous minerals, such as lawsonite, can crystallize as pressure and temperature are increased during subduction.

Lawsonite is particularly interesting for its high H_2O content (11.5 wt.%), water being present as both H_2O molecules and OH groups. The structure of lawsonite at ambient pressure and temperature, including likely positions of H atoms, was refined by Baur (1978). He described it in space group *Ccmm*. However, following convention, in this study we use the space group *Cmcm*, with $a \approx 5.85$ Å, $b \approx 8.79$ Å, $c \approx 13.14$ Å. The structure consists of chains of edge-sharing AlO_6 octahedra parallel to [100], linked by Si_2O_7 groups parallel to [001]. There are large cavities in the structure, occupied by one Ca atom and one H_2O molecule per formula unit. There are also two OH groups per formula unit, coordinated to Al.

* E-mail: alison.pawley@man.ac.uk

A number of recent experimental studies have suggested that lawsonite can persist in subducting oceanic crust to depths of hundreds of km (e.g. Pawley, 1994; Schmidt, 1995). Given the potential ultrahigh-pressure stability of lawsonite in the Earth, an understanding of the behaviour of its structure at high pressures is an important goal. The compressibility of lawsonite has been investigated in a number of recent studies, mostly using X-ray diffraction (XRD) to determine unit-cell parameters, and hence volume, as a function of pressure (and in some cases temperature). The results of these XRD studies are listed in Table 1. This table also shows whether the study used a natural or synthetic sample, whether the experimental apparatus was a diamond anvil cell (DAC) or multi-anvil apparatus (MA), the experimental technique used (energy-dispersive synchrotron powder diffraction, EDSPD, angle-dispersive synchrotron powder diffraction, ADSPD, or single-crystal diffraction using a conventional sealed-tube source, SCD), the highest pressure of data collection (P_{max}), and the method of pressure measurement. The values of room-temperature bulk modulus (K_{298}) shown are those obtained by the different authors by fitting a Birch-Murnaghan or Murnaghan equation of state (EOS) to the data with K' fixed at a value of 4. Where two values of K_{298} are shown, the study involved high-temperature as well as high-pressure measurements. The first value is from the room-temperature data only, the second from a Birch-Murnaghan fit of the room-temperature and high-temperature data together.

It is clear from Table 1 that a wide range in values of K_{298} has been obtained in previous studies on lawsonite, but there are no obvious explanations for the variation, e.g. type of sample or apparatus used, or experimental technique. The value obtained by Holland *et al.* (1996) is substantially greater than all of the others. Although the other two DAC studies give closer results, they still show a significant difference. The two MA studies show less difference, their bulk moduli falling between the DAC data. However, a comparison of the bulk moduli obtained from fits to the high-temperature and room-temperature data together reveal that they also show a difference well outside the combined uncertainty. There is no obvious explanation for this difference. Some of the discrepancies between previous results have, however, been explained before. The particularly high value obtained by Holland *et al.* (1996) is probably due to the use of too much sample leading to bridging of the sample between the diamonds and hence an underestimation of the compressibility. The same problem was identified in their measurements on zoisite (Pawley *et al.*, 1998). The difference between the other two DAC studies was ascribed by Daniel *et al.* (1999) to differences in pressure measurement, since Daniel *et al.* (1999) made a point of using a very small amount of sample to avoid bridging between the diamonds. Nevertheless, the range in results suggests some anomalous or unusual behaviour of lawsonite in some of these studies.

Unusual behaviour in lawsonite's equation of state has also been observed in two of the high-T studies. Daniel *et al.* (1999) inferred from their data that rather than the expected linear decrease in bulk modulus with temperature, as observed for most minerals, the bulk modulus of lawsonite begins to increase above ~500 K. Thus they were required to make d^2K_T/dT^2 non-zero in their Birch-Murnaghan fit. In contrast, Chinnery *et al.* (2000) noticed that an increase in bulk modulus from 298 to 373 K would be compatible with their data. This would explain the significant difference between the values of K_{298} obtained from the fit of the room-temperature data only and the fit of all of the data together. Therefore Chinnery *et al.* (2000) suggested that the compressibility measured at room temperature should not be used to calculate high-temperature behaviour.

Interesting behaviour has also been observed in lawsonite below room temperature. Libowitzky and Armbruster (1995) and Libowitzky and Rossman (1996) identified a phase transition at ~273 K in low-T, ambient-pressure, single-crystal XRD and infrared (IR) measurements on lawsonite. They observed that in the high-T *Cmcm* phase, the OH and H_2O in lawsonite are dynamically disordered about average positions. Below 273 K the hydrogen atoms order into asymmetric, static positions, and the symmetry is reduced to *Pmcn*. Another phase transition occurs at 150 K, where further shifts in the H positions lead to a phase with space group $P2_1cn$. Because high-P volume behaviour in minerals often mirrors that observed at low temperature (e.g. Hazen and Prewitt, 1977), it might be expected that these phase transitions would be observed on compressing lawsonite. Energy-dispersive X-ray powder diffraction cannot, however, be expected to distinguish between such structurally similar phases. The better resolution and useful peak

TABLE 1. Comparison of experimental conditions and results of compressibility measurements on lawsonite.

Study	Sample type	Apparatus	Experimental technique	P_{max} (GPa)	Pressure measurement	K_{298} (GPa)	dK_T/dT (GPa K^{-1})
Holland *et al.* (1996)	synthetic	DAC	EDSPD	12.0	NaCl	191(5)	–
Comodi *et al.* (1996)	natural	DAC	SCD	3.8	Sm^{2+}:BaFCl	96(2)	–
Daniel *et al.* (1999)	natural	DAC	ADSPD	7.8	ruby/NaCl*	124(2)/124(2)†	−0.111(3)**
Grevel *et al.* (2000)	synthetic	MA	EDSPD	6.8	NaCl	107(1)/106(4)‡	−0.020(7)
Chinnery *et al.* (2000)	natural	MA	EDSPD	6.8	NaCl	112(6)/125(5)	−0.01(1)
This study	natural	DAC	ADSPD	16.5	ruby	126.1(6)	–

* Ruby was used as a pressure calibrant at room temperature, NaCl at high temperature
† Where two values of K_{298} are shown, the second was obtained from a Birch-Murnaghan fit of room-T and high-T data together
** d^2K_T/dT^2 was allowed to vary in this Birch-Murnaghan fit. A value of $d^2K_T/dT^2 = 0.28(6)$ was obtained
‡ K' was allowed to vary in the second Birch-Murnaghan fit. A value of $K' = 4.7(17)$ was obtained (for constant thermal expansivity, $\alpha_{T,0}$)
See text for abbreviations and further explanation

intensity information provided by angle-dispersive diffraction, on the other hand, would be expected to allow these phase transitions to be observed. No transitions were observed, however, by Daniel *et al.* (1999) in their study up to 7.8 GPa, who saw no evidence for anything other than *Cmcm* symmetry.

The techniques employed by Daniel *et al.* (1999) up to 7.8 GPa have more recently been extended to 18 GPa at room temperature (Daniel *et al.*, 2000). In their paper they describe the existence of a phase transition at 8.6 GPa, which is different from the transitions described by Libowitzky and Armbruster (1995). Their paper was published while the current paper was in review. They observed a displacive phase transition between 7.8 and 8.7 GPa, from orthorhombic to monoclinic symmetry, identified by splitting of *hk*0 reflections in XRD patterns. They fitted their high-*P* data to the space group $C112_1/m$. This space group, which is conventionally represented as $P2_1/m$, was used so that the cell axes would remain approximately parallel to the *Cmcm* axes. They observed that across the transition the compressibility of the a parameter did not change, indicating that the Al octahedral framework of lawsonite is not involved in the phase transition. On the other hand, the compressibility of *b* and *c* decreased, suggesting a decrease in the compressibility of the cavities containing H_2O and OH.

Of the previous XRD studies, the only one to refine atomic positions at high pressure was that of Comodi and Zanazzi (1996). They refined the structure of lawsonite at ambient pressure, 0.05 and 2.87 GPa, and showed that the volume of the cavity containing the Ca atom and H_2O molecule compresses by only ~5% in this pressure range. At the same time, the Si—O—Si angle between tetrahedral pairs decreases, thus narrowing the cavities in the [001] direction.

Lawsonite has also been studied at high pressure using IR and Raman spectroscopy. Scott and Williams (1999) conducted an IR spectroscopic study to 20 GPa at 300 K, which examined the effects of pressure on vibrations of water molecules, hydroxyl groups and silicate tetrahedra. They used the band assignments of Libowitzky and Rossman (1996), who distinguished between two O—H bonds in both the H_2O molecule and OH group, each with a different stretching frequency (υ) due to different hydrogen bond strengths. A static, symmetrical *Cmcm* structure should have only one υOH, and two closely-spaced υH_2O, and so the occurrence of four O—H stretching bands was used by Libowitzky and Rossman (1996) as evidence of dynamic disorder of the H atoms about average positions in the *Cmcm* structure. On compression, Scott and Williams (1999) noted that both υOH changed rapidly up to 8—9 GPa (υOH(a) increased and υOH(b) decreased), where a discontinuity was observed, and above this pressure both frequencies decreased at a lower rate. This discontinuity was interpreted as being due to a pressure-induced change in H bonding. In contrast to the strong effects of pressure on the OH groups, both υH_2O and δH_2O (the H—O—H bending frequency) showed little change with pressure, and no discontinuity at 8—9 GPa, implying that the cavity containing the H_2O remains fairly rigid with pressure, the same conclusion as reached by Comodi and Zanazzi (1996) in their lower-pressure XRD study. The stretching and bending frequencies of the silicate groups showed continuous increases up to ~18 GPa. Therefore these units are also relatively unaffected by the discontinuity at 8—9 GPa. Interestingly, while the structural behaviour of phases with increasing pressure might be expected to be similar to their behaviour with decreasing temperature, the marked contrast between the small pressure shifts of the H_2O vibrations observed by Scott and Williams (1999) and the large temperature shifts observed by Libowitzky and Rossman (1996) shows that for lawsonite this similarity does not hold.

As well as XRD data, Daniel *et al.* (2000) collected Raman spectra of lawsonite up to 16 GPa. They came to the same conclusions regarding structural changes across the phase transition as did Scott and Williams (1999) from their IR study. These agreed with the conclusion from the XRD data that the aluminosilicate framework is not involved in the transition.

The studies discussed above, which produced some conflicting results in terms of the *P-V-T* behaviour of lawsonite and have shown some interesting structural discontinuities, prompted us to attempt a more detailed study of lawsonite's structural response to pressure using angle-dispersive synchrotron X-ray powder diffraction in a diamond anvil cell. We have measured the compressibility of lawsonite up to 16.5 GPa, refined the structure at high pressure, and investigated the response to heating to 200°C at 12 GPa. As in the study of Daniel *et al.* (2000),

which was published while our paper was in review, we observed a phase transition at high pressure, from orthorhombic to monoclinic symmetry.

Experimental technique

The sample of lawsonite came from a monomineralic vein in a blueschist from Jenner, California. It is the same sample as was used in the *P-V-T* study of Chinnery *et al.* (2000), whose electron microprobe analyses showed it to be essentially pure lawsonite, with ~0.05 Fe and 0.03 Mg per formula unit.

The sample was ground to a very fine powder prior to loading into the diamond anvil pressure cells. Diamond anvil cells of the Merrill-Bassett design were used as they provide full conical X-ray apertures with a 50° half angle. The diamond anvils had either 600 μm or 400 μm culets and the pre-indented tungsten gaskets had spark-eroded holes of 150 μm diameter. Samples were loaded with a 4:1 mixture of methanol/ethanol as a pressure-transmitting medium, and the pressure was measured to 0.1 GPa using the ruby fluorescence technique. Diffraction data were collected on station 9.1 at the Synchrotron Radiation Source, Daresbury Laboratory, at a wavelength of 0.4654 Å. The incident beam was collimated by a platinum pinhole to a diameter of 75 μm. The 2-dimensional powder patterns collected on the image plates were read on a Molecular Dynamics 400A PhosphorImager and then integrated using the PLATYPUS suite of programs (Piltz *et al.*, 1992) to give conventional 1-dimensional diffraction profiles. Details of the experimental setup and pattern integration software have been reported previously (Nelmes and McMahon, 1994). The integrated powder patterns were analysed using the Rietveld method with the GSAS refinement package (Larson and Von Dreele, 1994). We performed three high-*P* experimental runs on lawsonite, one of which was heated. The heated experiment was conducted by securing an external electrical resistive heater to the diamond-anvil cell. The sample temperature was monitored using a copper/constantin thermocouple attached to the gasket. The temperature uncertainty is estimated to be $\pm 2^{\circ}$C. For this experiment, the sample was mixed with NaCl, which acted as a pressure standard. This was required as the experimental set-up did not permit simultaneous heating and pressure measurement using ruby-fluorescence.

Results

Unit-cell refinements from our first two experimental runs are shown in Table 2, and structural details at selected pressures in the first run are shown in Table 3. In the first run we compressed the sample to 16.5 GPa, collecting diffraction patterns at intervals of ~2 GPa. The diffraction patterns showed no discernible changes up to 9.8 GPa (BN89) other than slight peak broadening due to internal stresses. At 9.8 GPa enhanced broadening was observed in two of the peaks (220 and 223) (Fig. 1), and an increase in the errors on derived structural parameters. The next diffraction pattern, at 11.9 GPa (BN90), showed clear differences from the lower-pressure patterns: peak splitting had occurred, and peak intensities had changed. These differences were enhanced as pressure was increased further. A final diffraction pattern collected at 3 GPa on decompression was similar to the low-pressure diffraction patterns collected during compression.

Up to 9.8 GPa, the data can be fitted by an orthorhombic cell with space group *Cmcm*, as in previous studies at low pressure, and in the study of Daniel *et al.* (2000) up to 8 GPa. Although peak broadening occurred at 9.8 GPa (BN89), the pattern was still best fit by an orthorhombic cell. The peak splitting from 9.8 to 11.9 GPa indicates that a phase transition has occurred between these two pressures. The new structure was fit by a monoclinic $P2_1/m$ cell. Figure 2*a* shows part of the Rietveld refinement of the monoclinic structure. In comparison, Fig. 2*b* shows the refinement of the same diffraction pattern as orthorhombic. The differences between observed and calculated profiles in Fig. 2*b* demonstrate that the orthorhombic refinement no longer provides the best fit. The *Cmcm* space group is a subgroup of the $P2_1/m$ space group, with $a_{ortho} = c_{mono}$, $b_{ortho} = 2a\sin\beta_{mono}$, $c_{ortho} = b_{mono}$ (Fig. 3). The change in assignment of cell axes from orthorhombic to monoclinic is required to maintain conventional notation. The monoclinic phase is derived from the orthorhombic phase by loss of the mirror plane parallel to (100) and the *c*-glide plane parallel to (010), and loss of orthogonality of a_{ortho} and b_{ortho}, as the sheets parallel to (010) which contain the AlO_6 octahedral chains are sheared relative to each other in the [100] direction, i.e. parallel to the lengths of the chains. These structural relationships will be discussed in more detail later.

TABLE 2. Unit-cell parameters and phase fractions of *Cmcm* and $P2_1/m$ phases of lawsonite.

Run number	Pressure (GPa)*	Space group	*a* (Å)†	*b* (Å)	*c* (Å)	β (°)	*V* (Å^3)	Phase fraction
BN Run								
BN82	0.0	*Cmcm*	5.849	8.790	13.132(1)		675.07(3)	
BN83	2.4(1)	*Cmcm*	5.813	8.727	13.054(1)		662.28(3)	
BN84	4.2(1)	*Cmcm*	5.785	8.684	12.998		653.00(3)	
BN86	5.7(1)	*Cmcm*	5.766	8.655	12.961(1)		646.72(3)	
BN88	8.3(1)	*Cmcm*	5.732	8.611	12.897(1)		636.51(3)	
BN89	9.8(4)	*Cmcm*	5.714(1)	8.592(1)	12.871(1)		631.85(6)	
BN90	11.9(3)	$P2_1/m$‡	5.197(1)	12.863(2)	5.681(1)	124.48(1)	313.10(3)	
BN94	14.6(2)	$P2_1/m$	5.188(1)	12.819(2)	5.649(1)	124.62(1)	309.15(3)	
BN97	16.5(2)	$P2_1/m$	5.178(1)	12.787(2)	5.634(1)	124.67(1)	306.82(3)	
BQ Run								
BQ85	0.0	*Cmcm*	5.851	8.794(1)	13.140(1)		676.08(5)	
BQ87	8.7(1)	*Cmcm*	5.733	8.613(1)	12.903(1)		637.14(4)	
BQ89	9.6(1)	*Cmcm*	5.722	8.599(1)	12.885(1)		634.05(4)	
BQ92	10.1	*Cmcm*	5.725(1)	8.601(1)	12.895(2)		634.97(9)	0.68
	10.1	$P2_1/m$	5.211(1)	12.887(1)	5.726(2)	124.04(2)	318.63(9)	0.32
BQ94	10.4	*Cmcm*	5.729(1)	8.604(1)	12.897(2)		635.66(9)	0.55
	10.4	$P2_1/m$	5.220(1)	12.920(2)	5.714(1)	124.35(1)	318.12(3)	0.45
BQ96	10.7(1)	*Cmcm*	5.717(1)	8.595(2)	12.880(3)		632.9(2)	0.42
	10.7(1)	$P2_1/m$	5.214(1)	12.909(2)	5.698(1)	124.47(1)	316.16(3)	0.58
BQ97	11.3(1)	*Cmcm*	5.712(1)	8.579(2)	12.859(2)		630.1(1)	0.31
	11.3(1)	$P2_1/m$	5.213(1)	12.893(1)	5.686(1)	124.48(1)	315.02(2)	0.69
BQ104	13.0	$P2_1/m$	5.200(1)	12.851(1)	5.665(1)	124.56(1)	311.80(2)	

* Pressures shown are averages of those measured before and after the scan. Errors are half of the difference between the two measurements

† No errors in cell parameters are shown where they are <0.0005 Å

‡ The relationship between the orthorhombic phase and the monoclinic phase is: $a_{ortho} = c_{mono}$, $b_{ortho} = 2a\sin\beta_{mono}$, $c_{ortho} = b_{mono}$

In our second run we took the pressure close to the pressure of the phase transition, and then collected diffraction patterns at much narrower pressure intervals across the transition. The highest-*P* experiment below the transition pressure was at 9.6 GPa (BQ89), where the diffraction pattern is similar to that obtained in the previous run (BN89). The following four experiments produced diffraction patterns that could only be refined as mixed *Cmcm* and $P2_1/m$ phases. Figure 4*a* shows the refinement of one of these diffraction patterns (BQ94) as a mixed phase, while Fig. 4*b* demonstrates that fitting only a monoclinic phase results in large differences between observed and calculated profiles. Only in the final experiment (BQ104), at 13.0 GPa, was single phase $P2_1/m$ lawsonite observed. Refined phase proportions calculated for the mixed-phase region are given in Table 2.

Results from these two experimental runs suggest that the phase transition in lawsonite is displacive, as it occurs rapidly and the sample transforms back to the low-*P* phase on decompression, and also that it is first order. This is indicated by the fact that a mixed-phase region was observed in the second experimental run, spanning >1 GPa. Through this interval the proportion of *Cmcm* lawsonite decreased as the proportion of $P2_1/m$ lawsonite increased (Table 2). Such a pressure region, in which parts of the sample have transformed while others have not, is commonly observed for first order phase transitions. In contrast, for second order transitions the change would be expected to be smooth and progressive.

It is unfortunate that the phase transition in lawsonite occurs close to the pressure at which methanol/ethanol freezes, and so the volume data from the BQ run are unable to provide any

TABLE 3. Atomic fractional coordinates of lawsonite as a function of pressure.

		BN82 0.0 GPa	BN89 9.8 GPa		BN90 11.9 GPa	BN97 16.5 GPa
x	Ca	0	0	Ca	0.310(3)	0.277(3)
y		0.3359(6)	0.333(1)		0.75	0.75
z		0.25	0.25		0.660(3)	0.649(3)
x	Al	0.25	0.25	Al1	0.5	0.5
y		0.25	0.25		0	0
z		0	0		0	0
x				Al2	0.5	0.5
y					0	0
z					0.5	0.5
x	Si	0	0	Si	0.934(2)	0.937(3)
y		0.9857(6)	0.9846(9)		0.1326(6)	0.1320(7)
z		0.1262(4)	0.1273(6)		0.939(2)	0.944(3)
x	O1	0	0	O1	0.824(8)	0.842(8)
y		0.046(1)	0.069(2)		0.75	0.75
z		0.25	0.25		0.842(7)	0.905(8)
x	O2	0.2780(9)	0.275(2)	O2	0.755(4)	0.767(4)
y		0.3815(7)	0.381(1)		0.120(2)	0.115(2)
z		0.1130(4)	0.1219(6)		0.670(5)	0.685(5)
x				O3	0.812(8)	0.894(5)
y					0.394(2)	0.392(2)
z					0.203(5)	0.255(4)
x	O3	0	0	O4	0.274(6)	0.279(7)
y		0.153(1)	0.169(2)		0.068(1)	0.075(2)
z		0.0589(6)	0.051(1)		0.159(4)	0.169(6)
x	O4	0	0	O5	0.290(4)	0.258(4)
y		0.6359(9)	0.625(1)		0.058(1)	0.056(2)
z		0.0469(7)	0.053(1)		0.630(4)	0.625(4)
x	O5	0	0	O6	0.734(7)	0.702(9)
y		0.600(2)	0.592(2)		0.75	0.75
z		0.25	0.25		0.298(7)	0.258(9)

information regarding volume discontinuity at the phase transition. Also, in the mixed-phase region, uncertainties in the refined structural parameters have led to considerable scatter in the calculated unit-cell parameters and volumes.

In our third run we took the sample straight up to a pressure of 15.3 GPa, collected a diffraction pattern to confirm that the sample had transformed to the high-pressure phase, and then heated it to 200°C. We collected a diffraction pattern at this temperature and at 50° intervals on cooling to room temperature. The pressure, measured from the ruby when the sample had cooled to room temperature, was 11.2 GPa. This substantial pressure drop on heating was not unexpected, as the relatively small loading force required to achieve high pressures in a diamond anvil cell is easily lost as a result of the small thermal expansion experienced by the cell during even a relatively small temperature increase.

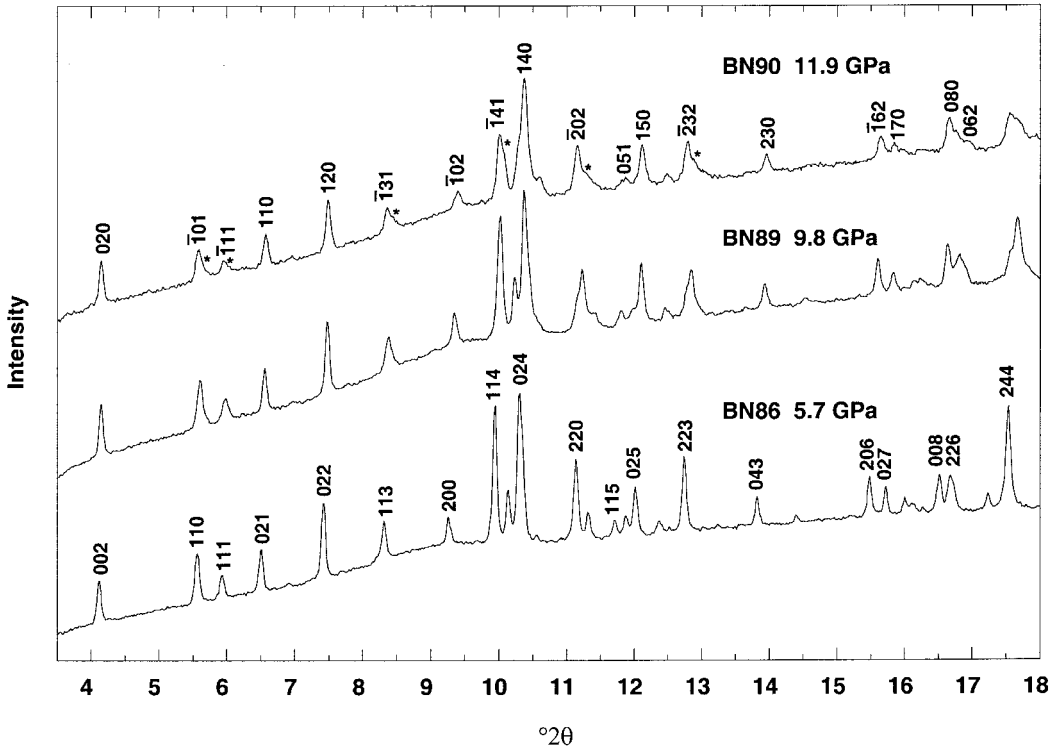

FIG. 1. Selected region of the diffraction patterns of lawsonite at three pressures. BN88 and BN89 are indexed according to the *Cmcm* cell, BN90 according to the $P2_1/m$ cell. Indicated with asterisks in the BN90 pattern are the less intense 0*kl* peaks of each pair of split peaks. The intensity scales are not the same for all three patterns.

Examination of the diffraction patterns showed that, unfortunately, the NaCl had dissolved in the pressure-transmitting medium at high temperature, and so we could not measure accurately the pressure in the high-*T* experiments. However, the diffraction patterns remained essentially unchanged as the temperature was reduced, indicating that the sample had followed an isochore (line of constant volume).

Compressibility of lawsonite

The unit-cell parameters obtained from the structural refinements in our first experimental run have been used to determine the compressibility of the low-pressure, orthorhombic, phase of lawsonite (Table 2 and Fig. 5). A Birch-Murnaghan equation, was fitted to the *Cmcm* volume data, with K' fixed at 4. This is a common practice where the number of data-points is limited, and reduces the Birch-Murnaghan equation to the form

$$P = \frac{3}{2}K_0\left[\left(\frac{V_0}{V}\right)^{\frac{7}{3}} - \left(\frac{V_0}{V}\right)^{\frac{5}{3}}\right]$$

From this fit we obtain V_0 = 674.5(1) Å^3, K_{298} = 126.1(6) GPa (assuming room temperature to be 298 K). The points plotted in Fig. 5 have been normalized to this value of V_0. Figure 5 also shows the relative compression of the individual cell parameters, normalized to their values at ambient pressure. It can be seen that orthorhombic lawsonite's compressibility is almost isotropic, with *c* being slightly less compressible than *a* and *b*.

The monoclinic cell parameters and volumes have not been included in Fig. 5 because the volumes appear to be too high relative to an extrapolation of the orthorhombic volumes to

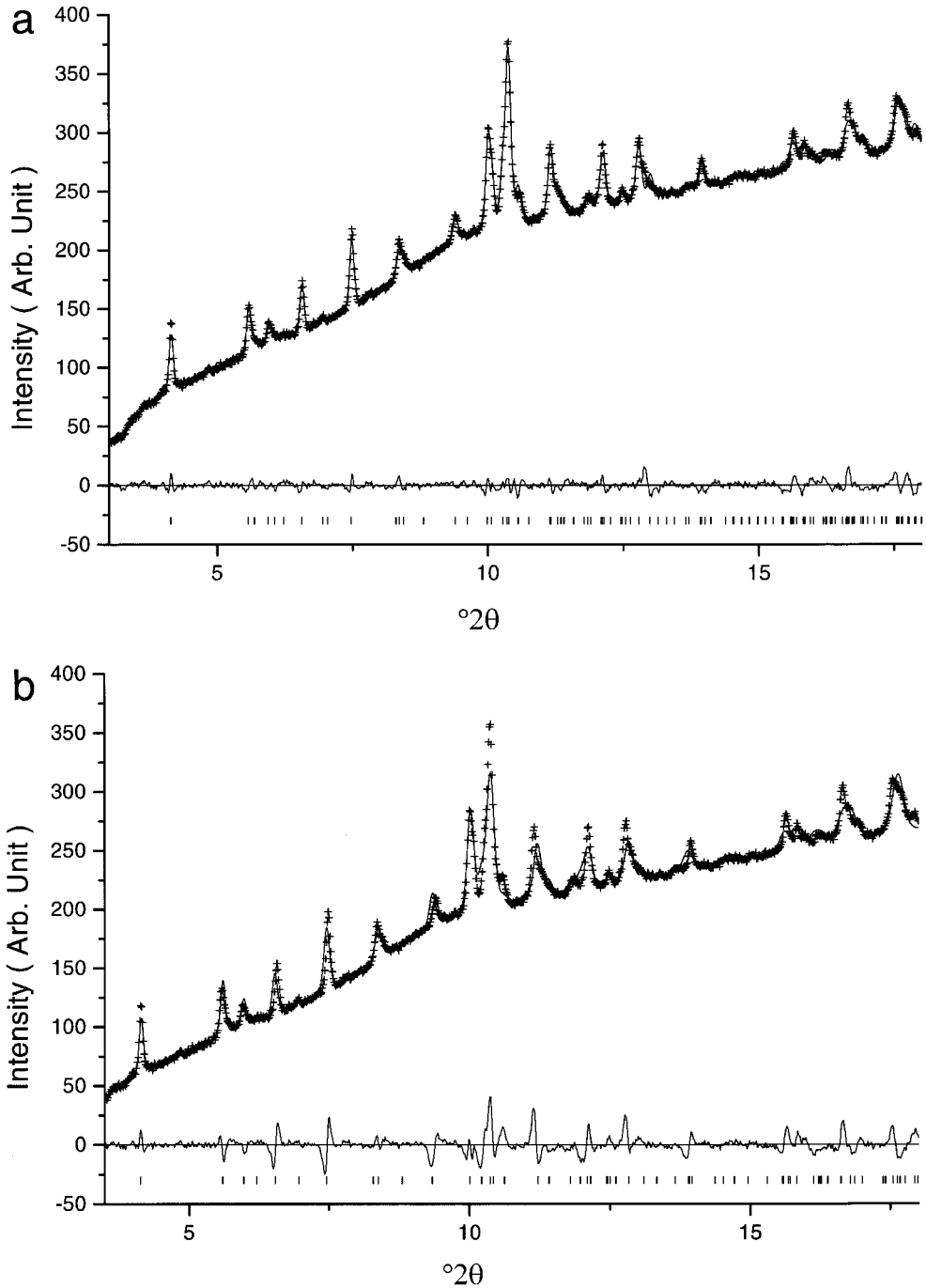

FIG. 2. Comparison of a selected region of the Rietveld refinements of lawsonite at 11.9 GPa (BN90), refined as: (*a*) monoclinic ($P2_1/m$); and (*b*) orthorhombic (*Cmcm*). The tick marks show the positions of all the reflections allowed by symmetry. The difference between the observed and calculated profiles is displayed above the tick marks. The region of 2θ shown is the same as in Fig. 1.

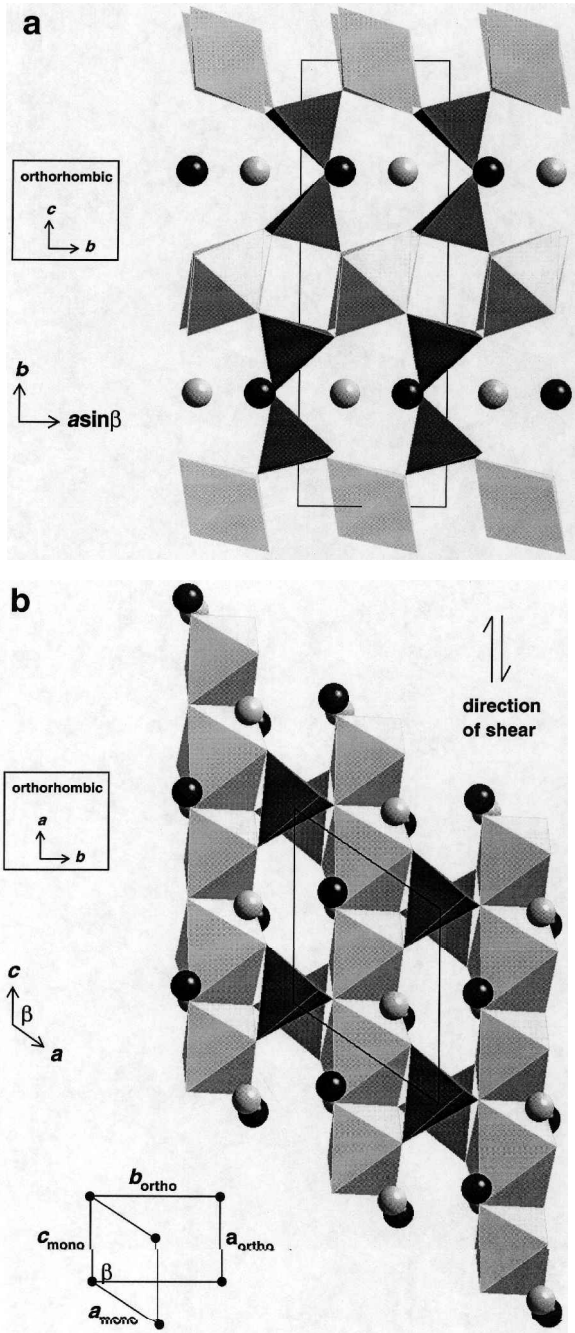

FIG. 3. Structure of $P2_1/m$ lawsonite (BN90, 11.9 GPa) viewed: (*a*) along [001]; and (*b*) along [010]. The insets show the equivalent *Cmcm* axes. Also shown in (*b*) are the direction of shearing associated with the phase transition (⇅), and the relationship between the C-face centred orthorhombic cell and the primitive monoclinic cell. Dark tetrahedra = SiO_4, light octahedra = AlO_6, dark spheres = H_2O, light spheres = Ca. (The structures were generated using CrystalMaker 4.0, D. Palmer, 1999.)

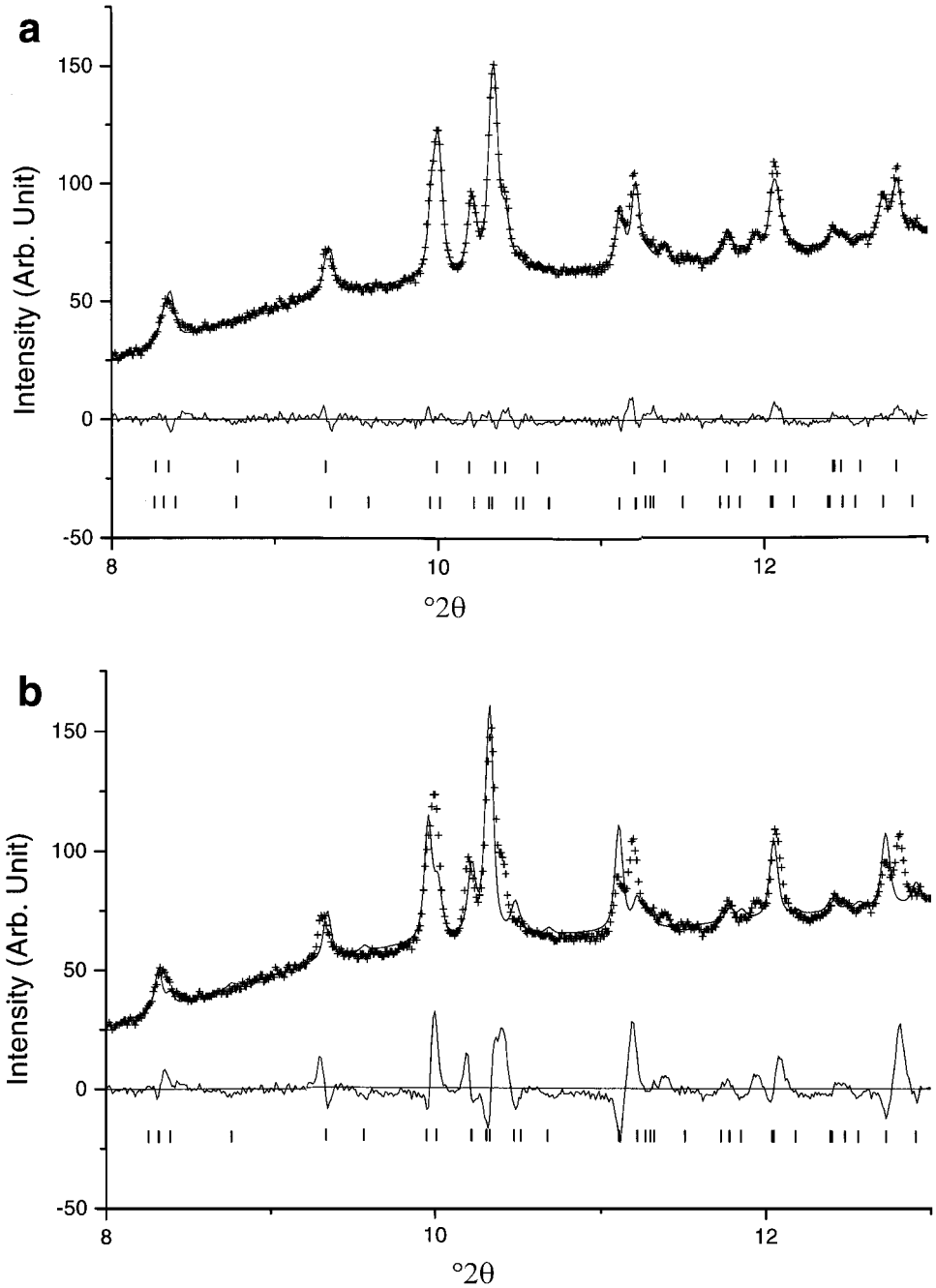

FIG. 4. Comparison of a selected region of the Rietveld refinements of lawsonite at 10.4 GPa (BQ94), refined as: (*a*) both orthorhombic (*Cmcm*) and monoclinic ($P2_1/m$); and (*b*) only monoclinic. The tick marks show the positions of all the reflections allowed by symmetry. The difference between the observed and calculated profiles is displayed above the tick marks. Note that for the fit with only the monoclinic phase, the cell dimensions, structural parameters and profile peak shapes were fixed at their values for the mixed phase refinement.

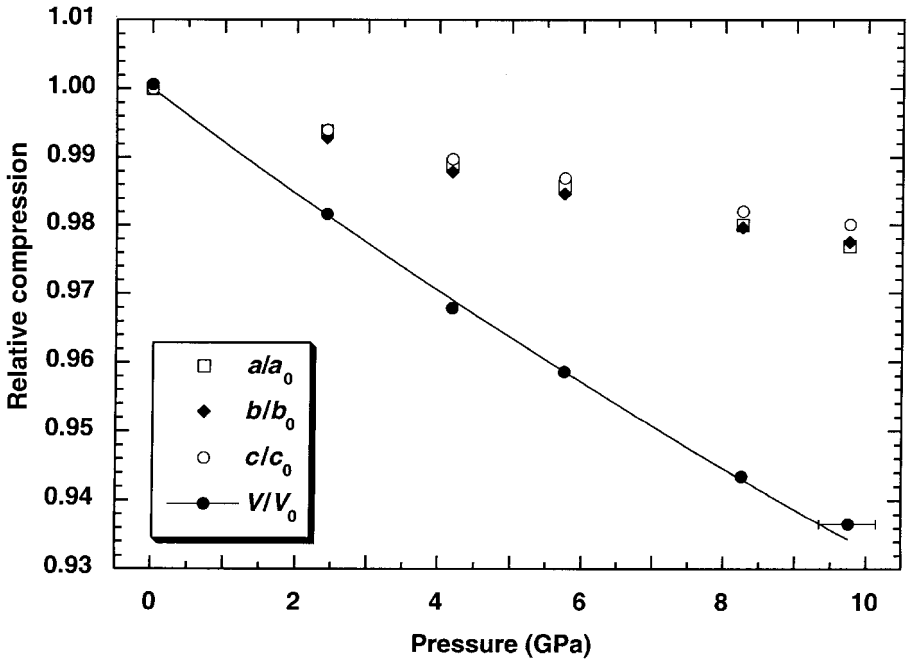

FIG. 5. Compressibility of the *Cmcm* phase of lawsonite. The curve is a fit of the Birch-Murnaghan equation to the volume data, with $K' = 4$, and normalized to the 0 GPa value obtained in the fit. Unit-cell parameters are normalized to the ambient-pressure values. Errors in pressure are taken from Table 2; errors in cell parameters and volumes are smaller than the symbols.

higher pressure. This is probably due to the solidification of the methanol/ethanol pressure-transmitting medium at ~10 GPa no longer providing a hydrostatic sample environment. This problem has been observed before in compressibility studies using methanol/ethanol (e.g. Brunet *et al.*, 1999). Thus we cannot determine the bulk modulus of the monoclinic phase. However, we can compare compressibilities of the individual cell axes, if we assume that their relative compressibilities are not affected by freezing of the pressure medium. The monoclinic cell parameters are plotted in Fig. 6, together with the orthorhombic parameters recast as monoclinic. The parameters are normalized to values at ambient pressure. Notable features of this figure are: (1) The angle β, which can be calculated from the orthorhombic cell parameters from $\tan(\beta-90) = a/b$, remains essentially constant in the orthorhombic phase as a_{ortho} and b_{ortho} compress equally, but then increases (by ~0.7%) at the phase transition as the orthorhombic symmetry is lost; (2) The shearing of the structure, through displacement of the AlO_6 octahedral chains parallel to their length, leads to an increase in a_{mono} as the structure is stretched out in this direction, but a steady decrease in $a\sin\beta$, the separation of the chains perpendicular to (100) (Fig. 3).

Structural changes across the phase transition

Some aspects of the structural changes associated with the phase transition are evident from the change in space group and cell parameters, as described in the previous section, most notably the shearing of the structure parallel to the AlO_6 octahedral chains, which opens up the angle β (Fig. 3). Other information may be obtained from the refined atomic positions from the Rietveld analysis. As for most Rietveld refinements, we anticipate that the errors on the fractional coordinates are underestimated. The reason for this is that whereas in single-crystal diffraction the observations (i.e. the Bragg intensities) are used directly in the refinement of the structural model and the errors on the fractional coordinates can be determined in a statistically rigorous and

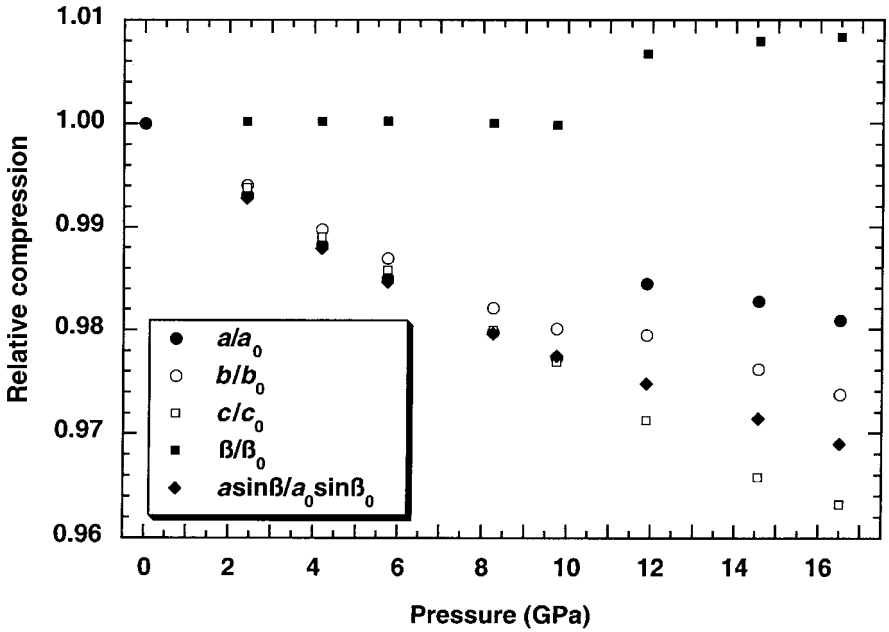

FIG. 6. Compressibility of cell parameters of $P2_1/m$ lawsonite, including the *Cmcm* parameters recast as $P2_1/m$. Note that $a_{ortho} = c_{mono}$, $b_{ortho} = 2a\sin\beta_{mono}$, $c_{ortho} = b_{mono}$. Data are normalized to the ambient-pressure measurements.

straightforward manner from the least-squares process, for Rietveld refinement the observations are not strictly the Bragg intensities but rather the individual points in the profile. To extract the diffracted intensities from the profile requires the involvement in the fit of other refinable parameters, such as peak shape parameters, background coefficients and lattice parameters, which all have associated errors. As the extracted diffracted intensities, which may also be highly correlated owing to peak overlap, do not include all sources of error, the estimated standard deviations on the structural parameters are generally underestimated. Therefore we expect that atomic positions will have rather large uncertainties. Nevertheless, some useful information can be obtained from examining variations in bond angles, bond lengths and polyhedral volumes with pressure.

Figure 7 shows Si—O—Si and Al—O—Si angles as a function of pressure for the BN run. There is considerable scatter in the Si—O—Si angle data (the derived errors are almost certainly underestimated, as explained above), and so we can only comment on the general trend of the data throughout the pressure range of study. A general decrease in this angle is apparent throughout compression. Thus the cavities containing the Ca and H_2O are narrowed in the direction of c_{ortho} (b_{mono}) by decreasing the angle between the SiO_4 tetrahedral pairs. The same behaviour was observed by Comodi and Zanazzi (1996).

The behaviour of the Al—O—Si angles is more complicated, as the number of symmetrically inequivalent Al sites increases from one to two across the transition. In the orthorhombic structure each SiO_4 tetrahedron is linked to two edge-sharing AlO_6 octahedra in one chain through two O2 oxygens, and linked to another octahedral chain through one O3 oxygen. In the monoclinic phase, Al1 and Al2 alternate along the chains, the two $O2_{ortho}$ oxygens become $O2_{mono}$ and $O3_{mono}$, and so $O3_{ortho}$ is renamed $O4_{mono}$. Figure 7 suggests that $Al—O2—Si_{ortho}$ and $Al—O3—Si_{ortho}$ both decrease a little during compression of the orthorhombic structure, probably due to compression of the structure in the [001] direction. On transforming to the monoclinic phase the shearing of the structure breaks the symmetry of the Al—O—Si angles and doubles their number. Rotation of the SiO_4 tetrahedra about $[010]_{mono}$ then leads to an increase in one of the formerly

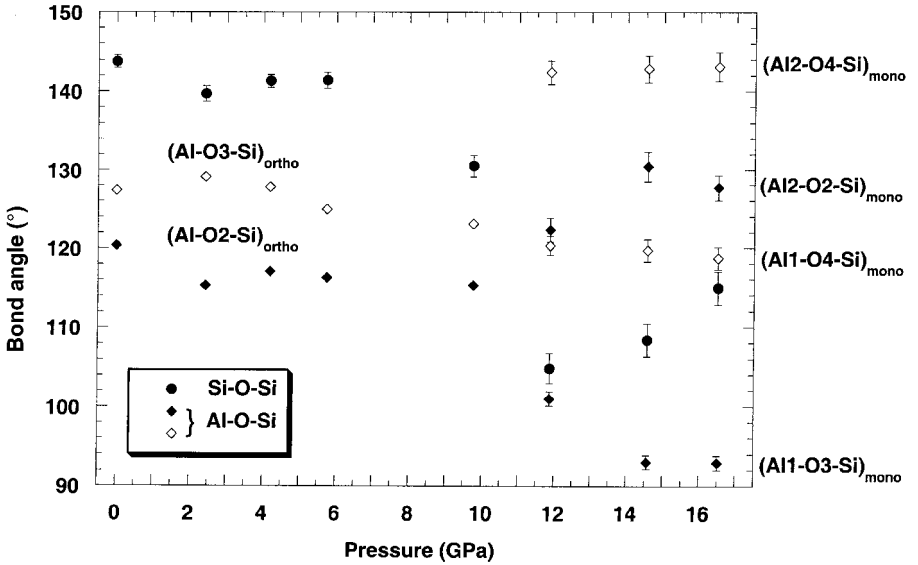

FIG. 7. Variation of lawsonite bond angles with pressure for the BN run. Note that BN88 has not been included in this plot or in Fig. 8, as there was a considerable amount of noise in its diffraction pattern, which had a shortened exposure owing to loss of the synchrotron beam.

Al—O2—Si_{ortho} angles and a decrease in the other (Al2—O2—Si_{mono} and Al1—O3—Si_{mono} respectively). Of the formerly Al—O3—Si_{ortho} angles, one continues to decrease smoothly from the orthorhombic values, while the other increases due to the shearing (Al1—O4—Si_{mono} and Al2—O4—Si_{mono} respectively)

Average bond lengths and polyhedral volumes have also been calculated for the coordination polyhedra of Si, Al and Ca in the BN run (the latter using the program VOLCAL, R.J. Angel, pers. comm.). Errors on the volumes are estimated to be quite large, particularly for the monoclinic phase (up to ~2.5%), as the volumes depend on the positions of each atom in the coordination polyhedron. Variation is, however, relatively smooth up to 6 GPa, over which pressure interval the SiO_4 tetrahedra and AlO_6 octahedra are both relatively incompressible, with neither bond lengths nor polyhedral volumes showing much variation. At higher pressure, scatter in the data obscures any obvious effect of the phase transition on the SiO_4 tetrahedra, but it is not expected that their compressibility will change significantly. The volume of one of the AlO_6 octahedra (Al1) apparently increases at the phase transition, but this may be a result of uncertainty in the derived oxygen positions, as there is no good crystal-chemical reason for such an increase. The Ca coordination environment shows more interesting behaviour (Fig. 8). In orthorhombic lawsonite, Ca can be considered as occupying a distorted octahedral site, with bonds to O1, O5 (the H_2O oxygen) and $4 \times O2$. There are also $2 \times O3$, with bonds to Ca at < 3 Å, which can be considered to be in the coordination sphere. The same oxygens are coordinated to Ca in the monoclinic structure, only renumbered to take into account the splitting of the O2 position. The variation of the average Ca—O bond lengths with pressure is interesting because both the average of 6 and the average of 8 increase across the transition. This may be due to an increase in coordination of the Ca from 8 to 9, as another O6 (= $O5_{ortho}$) enters the coordination sphere at a distance of 2.990 Å in BN90. Increases in bond distances across high-pressure phase transitions have been observed before, and interpreted as arising from an increase in coordination (e.g. gillespite, Hazen and Finger, 1983). The volume of the 8-fold coordinated Ca site shows a steady decrease from ambient pressure, through the phase transition. The bulk modulus of this site, calculated as the reciprocal of its linear compressibility up to 12 GPa, is 65 GPa. Thus this site is approximately twice as compressible as the structure as a whole, showing that

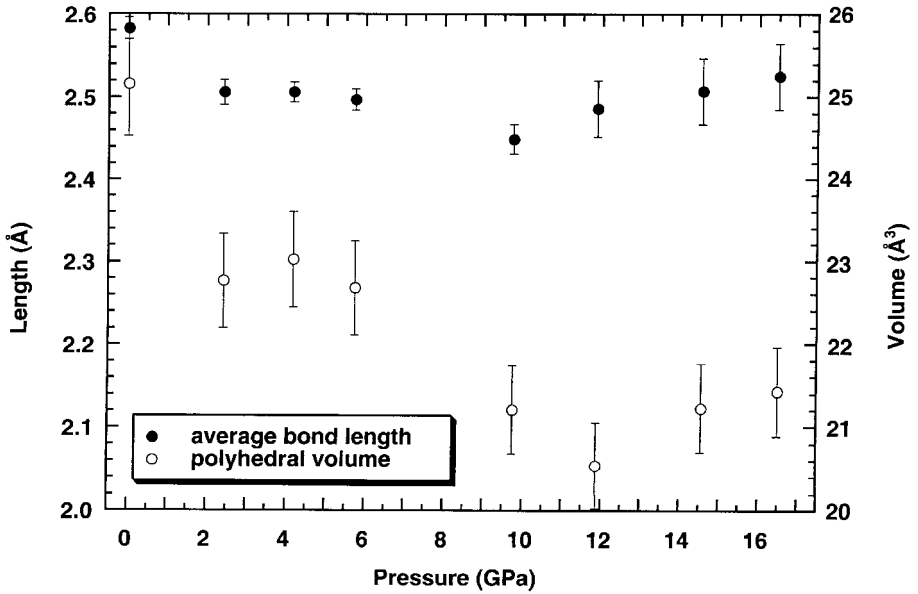

FIG. 8. Variation of average $(Ca-O)_8$ bond length and polyhedral volume with pressure for the BN run. The $(Ca-O)_6$ lengths and volumes show similar behaviour.

much of the volume compression is taken up by compression of this site, as expected for such a relatively large cavity. The bulk modulus of the 6-fold coordinated Ca site is similar to that of the 8-fold site: 62 GPa. This value is significantly smaller than that measured by Comodi and Zanazzi (1996), who obtained a bulk modulus of 114 GPa for the distorted CaO_6 octahedron.

High-*T* results

We have not attempted to refine the structures in our heated run, because of the pressure and temperature uncertainties associated with being close to the conditions of freezing of methanol/ethanol, and the NaCl dissolving in the methanol/ethanol. However, from the fact that on cooling from 200°C at unknown pressure, to room temperature at 11.2 GPa, we saw essentially no change in the diffraction patterns, we can say two things: the pressure at 200°C was not much greater than 11.2 GPa, and the structure was monoclinic over this *P-T* range. We can estimate the pressure at 200°C along an isochore, using the compressibility of lawsonite at room temperature obtained in this study, its thermal expansivity measured by Pawley *et al.* (1996), and dK_T/dT determined by Chinnery *et al.* (2000). From this calculation we obtain a pressure at 200°C of 12.0 GPa. Of course this is subject to some uncertainty, due to factors such as the possible freezing of the methanol/ethanol, the fact that the volume measurements were made on orthorhombic lawsonite, not the high-pressure monoclinic phase, and the uncertainties associated with the measurements of thermal expansivity and dK_T/dT. The fact that the monoclinic phase was observed on decompression to 11.2 GPa (at room temperature) contrasts with the observation of a mixed phase in run BQ97, at 11.3 GPa. This difference suggests that there is some hysteresis in the phase transition. It is, however, possible that the pressure uncertainties associated with the freezing of the methanol/ethanol pressure medium have led to inaccurate pressure estimates. If there is hysteresis at room temperature, then it might also be expected at 200°C, so that at this temperature the transition actually occurs at a higher pressure than we estimate, since we approached it from the high-pressure side.

Comparison with previous studies

Our value of the bulk modulus of lawsonite is essentially the same as determined in two previous studies (Table 1). This value is at the

high end of the range of previous measurements, excluding the anomalously high value of Holland *et al.* (1996). Our study does not shed any light on the reasons for the range in compressibilities previously reported. Although the measurements of Holland *et al.* (1996) extended above 10 GPa, any errors on the high-P data associated with the assumption of an orthorhombic structure would have had little effect on the derived bulk modulus. Our observation of no change in diffraction patterns up to a pressure of ~9 GPa agrees with the Daniel *et al.* (1999) study. As in their study, we saw no evidence for the low-T phase transitions observed by Libowitzky and Armbruster (1995). Those transitions were not associated with any volume discontinuity, but we would expect to be able to detect the transitions from changes in peak intensities. If the changes observed by Libowitzky and Armbruster (1995) and Libowitzky and Rossman (1996) do occur as pressure is increased, i.e. locking of hydrogen atoms into fixed positions rather than being dynamically disordered, then these presumably do not affect the rest of the structure sufficiently to make any impression on structural refinements. X-ray diffraction cannot itself identify H positions, and so we cannot rule out such changes occurring.

Our results are in very good agreement with those of Daniel *et al.* (2000). The unit cell we determined for the monoclinic high-P phase is essentially the same as theirs (though they transformed the cell from conventional $P2_1/m$ symmetry to $C112_1/m$ symmetry). We also observed a decrease in the compressibility of b_{ortho} and c_{ortho} relative to a_{ortho} across the phase transition. However, our results do differ in that we have located the transition at a pressure more than 1 GPa greater than theirs, and we observed a mixed-phase region, leading us to infer that the transition is first order, in contrast to their conclusion that it is unlikely to be first order. Our results are based on the Rietveld refinements, so that although we observed peak broadening below 10 GPa, it did not have a significant effect on *Cmcm* refinements. Likewise, refinements of BQ92 to 97 were only possible as mixed-phase samples, as shown in Fig. 4. Without the Rietveld refinements, the occurrence of a mixed-phase region would not have been clear, and we would certainly not have been able to determine phase proportions through this region (Table 2).

Our values for the atomic fractional coordinates of lawsonite at ambient pressure can be compared with previous single crystal studies (Baur, 1978; Comodi and Zanazzi, 1996). We note that our errors are greater, which is to be expected for refinement of powder diffraction patterns. We have already noted that these errors are almost certainly underestimated, and we assume that this explains the fact that our atomic positions do not agree with the previous positions within error. The conclusions we draw from our Rietveld refinements are broadly consistent with the results of Comodi and Zanazzi (1996), in that we also observed narrowing of the cavities containing Ca and H_2O in the direction of c_{ortho}. Our study shows that this behaviour continues to pressures beyond those investigated by Comodi and Zanazzi (1996). We did, however, observe a greater compressibility for the Ca-O polyhedron than they did. However, our value is subject to considerable uncertainty, given the large errors on the polyhedral volume calculations.

Our results also complement the results of the IR study of Scott and Williams (1999). They observed discontinuities in υOH at 8–9 GPa, slightly lower than our transition pressure of 10–11 GPa, but only smooth behaviour in υH_2O and δH_2O. This is consistent with the cavities containing Ca and H_2O showing a smooth volume change, within error, across the phase transition, while the OH groups, in the narrow channels between bases of neighbouring SiO_4 tetrahedral pairs, are clearly more strongly affected by the shearing of the structure and rotation of these SiO_4 groups.

P-T position of lawsonite phase transition

Combining the results of our three experimental runs, we infer that the phase transition in lawsonite occurs at 10–11 GPa at room temperature, and probably at no more than 12 GPa at 200°C. This high-T point is a poor constraint on the P-T slope of the phase transition, but we might also predict a positive slope, so that increasing pressure has the same effect on the structure as decreasing temperature (Hazen and Finger, 1979). Thus a shallow positive P-T slope appears likely. If this is the case, then the monoclinic phase of lawsonite will not occur in the Earth, as shown by the relationship of the phase transition to experimentally-determined positions of lawsonite's breakdown reactions (Fig. 9). However, a negative slope cannot be ruled out, which would intersect the stability field of lawsonite.

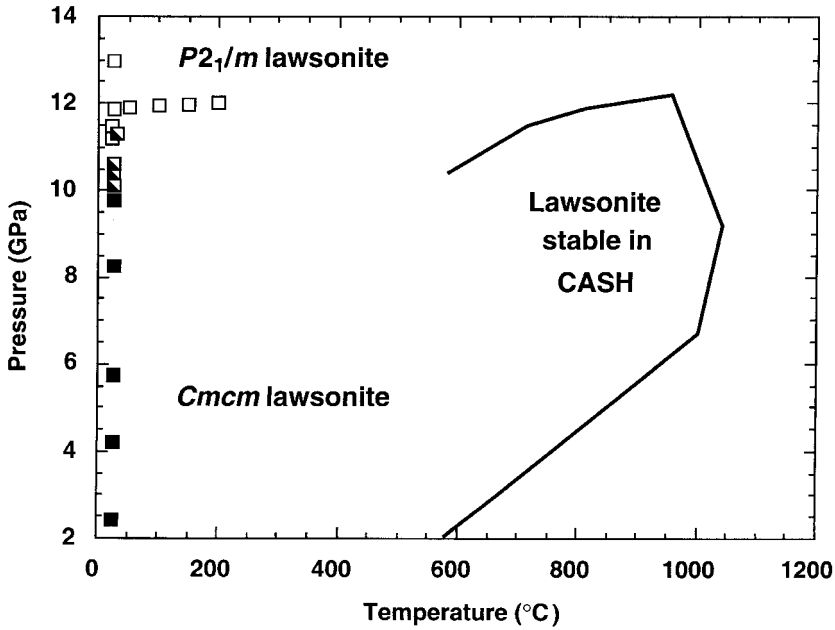

FIG. 9. Pressure-temperature points of our experiments, showing the stability fields of *Cmcm* lawsonite (filled symbols) and $P2_1/m$ lawsonite (open symbols) and the mixed-phase region (half-filled symbols). The high-*P,T* stability field of lawsonite in the system $CaO–Al_2O_3–SiO_2–H_2O$ determined by Schmidt (1995) is also shown.

Conclusions

Our high-pressure angle-dispersive synchrotron powder diffraction data of lawsonite compressed in a diamond anvil cell to 16.5 GPa show that the ambient *P,T* orthorhombic *Cmcm* structure is preserved up to 10 GPa, and apart from any undetectable changes of H positions, the structure compresses smoothly and relatively isotropically. The bulk modulus of the orthorhombic phase is 126.1(6) GPa (for $K' = 4$). Compression is accommodated partly through narrowing of the cavities containing Ca and H_2O in the [001] direction. At 10–11 GPa there is a phase transition, to a monoclinic $P2_1/m$ structure. The transition occurs through the shearing of $(010)_{ortho}$ planes containing AlO_6 octahedral chains in the $[100]_{ortho}$ direction, thus removing the $(100)_{ortho}$ mirror plane and the orthogonality of the a_{ortho} and b_{ortho} axes. The main polyhedral angles to be affected by the transition are Al–O–Si angles, which are sensitive to displacements of AlO_6 octahedral chains relative to each other. Polyhedral volumes are not significantly affected by the transition, but the coordination to Ca increases, causing an increase of average Ca–O bond length. Cell volumes across the transition are not clear from this study, due to pressure uncertainties associated with freezing of the methanol/ethanol pressure medium. The phase transition probably has a shallow positive *P-T* slope, and so the high-*P* monoclinic phase of lawsonite will in fact be metastable with respect to high-*P* breakdown products of lawsonite, e.g. grossular, stishovite, diaspore. However, further study of the transition at high temperature is required to verify that it does not intersect the stability field of lawsonite in the Earth. If it did, then calculations of lawsonite reactions based on thermodynamic data obtained from the orthorhombic phase would be in error.

Acknowledgements

This work was supported by Natural Environment Research Council grant GR3/11181 to ARP. We thank Malcolm McMahon, Scott Belmonte, Thiti Bovornratanaraks and Carine Vanpeteghem for help with experimental set-up, Lachlan Cranswick for help with data analysis, and Thiti Bovornratanaraks for help in preparing some of the figures. We thank K.D. Grevel and an

anonymous reviewer for useful comments on this paper.

References

Baur, W.H. (1978) Crystal structure refinement of lawsonite. *Amer. Mineral.*, **63**, 311–5.

Brunet, F., Allan, D.R., Redfern, S.A.T., Angel, R.J., Miletich, R., Reichmann, H.J., Sergent, J. and Hanfland, M. (1999) Compressibility and thermal expansivity of synthetic apatites, $Ca_5(PO_4)_3X$ with X = OH, F and Cl. *Eur. J. Mineral.*, **11**, 1023–35.

Chinnery, N.J., Pawley, A.R. and Clark, S.M. (2000) The equation of state of lawsonite to 7 GPa and 873 K, and calculation of its high pressure stability. *Amer. Mineral.*, **85**, 1001–8.

Comodi, P. and Zanazzi, P.F. (1996) Effects of temperature and pressure on the structure of lawsonite. *Amer. Mineral.*, **81**, 833–41.

Daniel, I., Fiquet, G., Gillet, P., Schmidt, M.W. and Hanfland, M. (1999) P-V-T equation of state of lawsonite. *Phys. Chem. Miner.*, **26**, 406–14.

Daniel, I., Fiquet, G., Gillet, P., Schmidt, M.W. and Hanfland, M. (2000) High-pressure behaviour of lawsonite: a phase transition at 8.6 GPa. *Eur. J. Mineral.*, **12**, 721–33.

Grevel, K.D., Nowlan, E.U., Fasshauer, D.W. and Burchard, M. (2000) In situ X-ray diffraction investigation of lawsonite and zoisite at high pressures and temperatures. *Amer. Mineral.*, **85**, 206–16.

Hazen, R.M. and Finger, L.W. (1979) Polyhedral tilting: A common type of pure displacive phase transition and its relationship to analcite at high pressure. *Phase Trans.*, **1**, 1–22.

Hazen, R.M. and Finger, L.W. (1983) High-pressure and high-temperature crystallographic study of the gillespite I-II phase tranistion. *Amer. Mineral.*, **68**, 595–603.

Hazen, R.M. and Prewitt, C.T. (1977) Effects of temperature and pressure on interatomic distances in oxygen-based minerals. *Amer. Mineral.*, **62**, 309–15.

Holland, T.J.B., Redfern, S.A.T. and Pawley, A.R. (1996) Volume behavior of hydrous minerals at high pressure and temperature: II. Compressibilities of lawsonite, zoisite, clinozoisite and epidote. *Amer. Mineral.*, **81**, 341–8.

Larson, A.C. and Von Dreele, R.B. (1994) GSAS, General Structure Analysis System. *Los Alamos National Laboratory, LAUR*, 86-748.

Libowitzky, E. and Armbruster, T. (1995) Low-temperature phase transitions and the role of hydrogen bonds in lawsonite. *Amer. Mineral.*, **80**, 1277–85.

Libowitzky, E. and Rossman, G.R. (1996) FTIR spectroscopy of lawsonite between 82 and 325 K. *Amer. Mineral.*, **81**, 1080–91.

Nelmes, R.J. and McMahon, M.I. (1994) High-pressure powder diffraction on synchrotron sources. *J. Synch. Radiat.*, **1**, 69–73.

Pawley, A.R. (1994) The pressure and temperature stability limits of lawsonite: Implications for H_2O recycling in subduction zones. *Contrib. Mineral. Petrol.*, **118**, 99–108.

Pawley, A.R., Redfern, S.A.T. and Holland, T.J.B. (1996) Volume behavior of hydrous minerals at high pressure and temperature: I. Thermal expansion of lawsonite, zoisite, clinozoisite, and diaspore. *Amer. Mineral.*, **81**, 335–40.

Pawley, A.R., Chinnery, N.J. and Clark, S.M. (1998) Volume measurements of zoisite at simultaneously elevated pressure and temperature. *Amer. Mineral.*, **83**, 1030–6.

Piltz, R.O., McMahon, M.I., Crain, J., Hatton, P.D., Nelmes, R.J., Cernik, R.J. and Bushnell-Wye, G. (1992) An Imaging Plate System for High-Pressure Powder Diffraction: The Data Processing Side. *Rev. Sci. Instrum.*, **63**, 700.

Schmidt, M.W. (1995) Lawsonite: upper pressure stability and formation of higher density hydrous phases. *Amer. Mineral.*, **80**, 1286–92.

Scott, H.P. and Williams, Q. (1999) An infrared spectroscopic study of lawsonite to 20 GPa. *Phys. Chem. Miner.* **26**, 437–45.

[*Manuscript received 3 May 2000: revised* 18 September 2000]